Research Article **RJMCS (2017) Vol. 1, Issue 01**

Research Journal of Mathematics and Computer Science (RJMCS)

Application of the Discrete Geometrical Invariants to the Quantitative Monitoring of the Electrochemical Background

R. R. Nigmatullin[1], H. C. Budnikov[2], A. V. Sidelnikov[3], E. I. Maksyutova[3]

[1]Radioelectronic and Informative-Measurements Techniques Department, Kazan National Research Technical University (KNRTU-KAI)K. Marx str. 10. , 420011, Kazan, Tatarstan, Russian Federation; [2]A.M. Butlerov Institute of Chemistry, Kazan Federal University (KFU), Kazan, Russian Federatio; [3]Chemistry Department, Bashkir State University, Ufa, Russian Federation

ABSTRACT

In this paper, we apply the statistics of the fractional moments (SFM) and discrete geometrical sets/invariants (DGI) for explain of the temporal evolution of the electrochemical background. For analysis of this phenomenon, we apply the internal correlation factor (ICF) and proved that integral curves expressed in the form of voltammograms (VAGs) are more sensitive in comparison with their derivatives. For analysis of the VAGs (integral curves), we propose the set of the quantitative parameters that form the invariant DGI curves of the second and the fourth orders, correspondingly. The method of their calculation based on the generalization of the well-known Pythagor's theorem is described. The quantitative parameters that determine these DGI allow monitoring the background of the electrochemical solution covering the period of 1-1000 measurements for two types of electrode (Pt and C) and notice the specific peculiarities that characterize each electrode material. The total set of 1000 measurements was divided on 9 parts (1-100, 101-200, 201-300, …, 901-1000) and the duration of each hundred set was 1300 sec. The proposed algorithm is sensitive and has a "universal" character. It can be applied for a wide set of random curves (experimental measurements) that are needed to be compared in terms of a limited number of the integer moments. The qualitative peculiarities of the background behavior for two types of electrodes (Pt and C) based on the DGI can be explained quantitatively.

Keywords: Application of the Discrete Geometrical Invariants, Quantitative Monitoring, Electrochemical Background

***Correspondence to Author:**
R. R. Nigmatullin
Radioelectronic and Informative-Measurements Techniques Department, Kazan National Research Technical University (KNRTU-KAI)
K. Marx str. 10. , 420011, Kazan, Tatarstan, Russian Federation

How to cite this article:
R. R. Nigmatullin et al., Application of the Discrete Geometrical Invariants to the Quantitative Monitoring of the Electrochemical Background. Research Journal of Mathematics and Computer Science, 2017; 1:7

.

eSciencePublisher
eSciPub LLC, Houston, TX USA.
Website: http://escipub.com/

1. Introduction and Formulation of the Problem

The phase boundary surface between electrode/solution is under the attention of many researches, working in the electroanalytical chemistry. This surface serves as a specific microreactor in which many temporal and electrochemical processes being under the controlled conditions give useful information about the electrode material, structure of the surface, about the components of the solution reacting in the depth of the solute and near the DEL (see for details the papers [1,2]).

The evolution of an analytical signal (or signals in the case of the electrode set usage), which is generated in this process contains full information. The selection of the proper equipment is determined by the aims and problems that can be solved in carrying out of this research. In the case of many-dimensional parameters that are appeared in the result of the multi-sensor electrodes usage, the corresponding mathematical treatment should be used. It can be associated with the hard or soft models [3, 4], accordingly. New materials and innovation technologies related to formation of the structural surfaces with the usage of different composites, supramolecular structures etc. require more informative and sophisticated methods for the various electrodes-sensors creation and taking into account other factors that can modify the given electrode in the stage of its production or in the process of its reaction with components of solution under investigation. From one side, a researcher has a variety of different sensitive equipment [5] however, from another side for the mathematical treatment of the data obtained and construction of the informative and effective models, new approaches are necessary. The most vital problem in this attention is related to description and quantitative characterization of the electrode surface in its continuous interaction with solution components. This problem is tightly related to creation of new generation of multi-sensor systems, which enable to detect all temporal changing in the process of its interaction with the solute under investigation. When the number of the measurements are rather small there are mathematical methods that take into account the drift of the detected signal in time [6] while for the multi-cycling sensor(the number of the measurement cycles are large, $M \geq 1000$) the mathematical methods related to quantitative monitoring of these sensors in time are not well developed. In this case, the electrode surface is changed significantly and can reflect the different stages of its electrochemical transformations [7, 8]. It is known that in the inverse voltamperometry for the receiving of the reproducible working electrode surface, it is polarized in the cycling regime for the chosen potential range. This experimental technique can be applied also for the sensor electrodes. The solution of the problem of the sensor control and its proper “aging” process parameterization in the condition of the continuous sensor functioning determines the reliability in detection of possible component traces [9]. It is known that the less dispersion of the background signals (but not their absolute values) extends the detection limit of an analyte. The state of the sensor/electrode surface in the result of extended temporal action can be determined as self-modification. It is necessary to describe the self-modification surface phenomenon by new methods because it has large fields of its possible application. It can be observed in the process of catalysts production, different sorbents, and porous composite materials and having, in turn, a practical importance in industry. It is known also that the creation of the fireproof materials includes the stage of electrochemical intercalation of the graphite in various media and the quality of the final product strongly depends on the duration of the electrochemical action on electrode, the nature of the background electrolyte, the values of the applied anode potentials and etc. [10]. The saying above put forward a problem related to

new and general mathematical method creation that can control quantitatively the evolution state of the electrode surface and expresses it in terms of the finite number of the given parameters. This method based on the usage of the discrete geometrical invariants (DGI) developed in this paper.

2. Description of the Method

2.1. *Preliminary considerations and the DGI of the second order*

In the books of Yu. I Babenko [11, 12] it was shown that the well-known Pythagoras theorem can be *generalized* and propagated for a set of random points having coordinates (x_k, y_k) (k=1,2,3…,n). Really, let us consider the square of the distance connecting an arbitrary point $M(x, y)$ with the k^{th} point (x_k, y_k) belonging to the given set

$$l_k^2 = \left(x - x_k\right)^2 + \left(y - y_k\right)^2, \tag{1}$$

We require that

$$\frac{1}{n}\sum_{k=1}^{n} l_k^2 = I^2 \equiv const\,. \tag{2}$$

Inserting expression (1) into (2), we obtain

$$\left(x - \langle x\rangle\right)^2 + \left(y - \langle y\rangle\right)^2 = I^2 - R^2,$$
$$\left\langle x^p\right\rangle = \frac{1}{n}\sum_{k=1}^{n} x_k^p,\ \left\langle y^p\right\rangle = \frac{1}{n}\sum_{k=1}^{n} y_k^p,\ R^2 = \left\langle \Delta x^2\right\rangle + \left\langle \Delta y^2\right\rangle,$$
$$\left\langle \Delta V^2\right\rangle = \left\langle V^2\right\rangle - \langle V\rangle^2. \tag{3}$$

As one can notice from (3) the set of circles can exist if the invariant $I^2 \geq R^2$, the equality sign corresponds to the circle with zero radius. For as, it is convenient to consider the invariant circle with radius $I^2=2R^2$. From another point of view, the requirement (2) can be considered as the reduction of the given set of points to the continuous circle with 4 statistical parameters (<x^p>, <y^p>, p=1,2). However, for practical purposes this simplest requirement (2) is *not* sufficient and therefore, it has sense to consider other geometrical combinations. In order to have reduction to the curve with eight statistical parameters, we consider another combination that is more complex in comparison with (1)

$$L_k^{(2)} = C^2\left(y - y_k\right)^2 - 2B\left(x - x_k\right)\cdot\left(y - y_k\right) + A^2\left(x - x_k\right)^2,$$
$$k = 1, 2, ..., n \tag{4}$$

The quadratic form (4) contains 5 statistical parameters (<x^p>, <y^p>, p=1,2; <xy>) and 3 unknown parameters (A,B,C) figuring in (4). We subordinate this combination to the requirement

$$\frac{1}{n}\sum_{k=1}^{n} L_k^{(2)} = I^2 \equiv const\,. \tag{5}$$

Inserting (4) into (5) after simple algebraic manipulations, one can obtain

$$C^2\left(y - \langle y\rangle\right)^2 - 2B\left(y - \langle y\rangle\right)\cdot\left(x - \langle x\rangle\right) + A^2\left(x - \langle x\rangle\right)^2 + E^2 \equiv I^2,$$
$$E^2 = C^2\left\langle \Delta y^2\right\rangle - 2B\left\langle \Delta x \Delta y\right\rangle + A^2\left\langle \Delta x^2\right\rangle. \tag{6}$$

As before, we put $I^2=2E^2$. In order to find three unknown parameters (A,B,C), it is convenient to use the obvious parameterization for the variables (x,y) relatively the angle φ

$$y = \langle y\rangle + A\cos\left(\varphi - \alpha\right),$$
$$x = \langle x\rangle + C\cos\left(\varphi\right),\ 0 \leq \varphi \leq 2\pi. \tag{7}$$

Excluding the parameter φ from (7) and identifying expression (6) with expression

$$C^2\left\langle (\Delta y)^2\right\rangle - 2AC\cos\alpha\left\langle (\Delta x)\cdot(\Delta y)\right\rangle + A^2\left\langle (\Delta x)^2\right\rangle \equiv A^2C^2 - B^2,$$
$$E^2 = C^2\left\langle \Delta y^2\right\rangle - 2AC\cos\alpha\left\langle \Delta x \Delta y\right\rangle + A^2\left\langle \Delta x^2\right\rangle = A^2C^2\sin^2\alpha, \tag{8}$$

we obtain

$$\cos\alpha = \frac{B}{AC},\ E^2 = A^2C^2 - B^2. \tag{9}$$

In order to decrease the number of unknown parameters, we find from (7) the values A and C from the obvious conditions:

$$y_{\max} = \langle y\rangle + A,\ y_{\min} = \langle y\rangle - A,\ \rightarrow A = \frac{1}{2}\left(y_{\max} - y_{\min}\right),$$
$$x_{\max} = \langle x\rangle + C,\ x_{\min} = \langle x\rangle - C,\ \rightarrow C = \frac{1}{2}\left(x_{\max} - x_{\min}\right). \tag{10}$$

Parameter B is found from relationships (8) and

(9) as a positive root of the quadratic equation written relatively *B*

$$B^2 - 2\langle \Delta x \Delta y \rangle B - \left[A^2 C^2 - \langle \Delta x^2 \rangle A^2 - \langle \Delta y^2 \rangle C^2 \right] = 0,$$

$$B = \langle \Delta x \Delta y \rangle + \left[\left(\langle \Delta x \Delta y \rangle \right)^2 + A^2 C^2 - \langle \Delta x^2 \rangle A^2 - \langle \Delta y^2 \rangle C^2 \right]^{1/2}. \quad (11)$$

This root is chosen from the comparison of two identity sequences ($x_k = y_k$) that follows from the obvious requirement $B=A^2$, (α=0). Concluding this section, one can say that with the help of the rotated counterclockwise ellipse (7) we reduced 2*n* random points figuring in (4) to 7 statistical parameters (<x^p>, <y^p>, *p*=1,2; <*xy*>, *A*, *C*). If it is necessary to include the higher moments <$x^p y^s$> (*p*=0,1,2,..; *s*=0,1,2…) then other combinations of the type (4) should be considered. Based on these preliminary considerations one can propose the basis of the DGI theory.

2.2. *The general theory of the geometrical invariants based on the higher order curves and the GDI of the forth order*

Unifying the ideas expressed in books [11, 12], one can consider the following combination

$$L_k^{(m)} = \sum_{q=0,\, p=0}^{m} A_{qp} \left(x - x_k \right)^q \left(y - y_k \right)^p . \quad (12)$$

This combination can be considered as the most *general* form that can be used for comparison of two random sets having coordinates (x_k, y_k) (*k*=1,2,3…,*n*). If one requires that

$$\frac{1}{n} \sum_{k=1}^{n} L_k^{(m)} = Inv , \quad (13)$$

then this form can be considered as the most general form for comparison of two random sequences of an arbitrary order in terms of different combinations of the integer moments. If we insert (12) into (13) and open the corresponding terms then we obtain possible combinations of the integer moments of the type

$$M_{qp} = \left\langle (\Delta x)^q (\Delta y)^p \right\rangle \equiv \frac{1}{n} \sum_{k=1}^{n} \left(x - \langle x \rangle - \Delta x_k \right)^q \left(y - \langle y \rangle - \Delta y_k \right)^p,$$

$$\langle A \rangle = \frac{1}{n} \sum_{k=1}^{n} A_k, \; \Delta A_k = A_k - \langle A \rangle. \quad (14)$$

In this section, having in mind its practical application for comparison of the different experimental data with each other we consider only the special invariant of the 4-th order that will be helpful for more fine comparison of two sets (in our case the comparison of the integral VAGs affected by the presence of some external factor). This combination allowing finding the desired invariant in the analytical form has a form

$$L_k^{(4)} = A_4 \left(x - x_k \right)^4 + 2B_4 \left(x - x_k \right)^2 \left(y - y_k \right)^2 + C_4 \left(y - y_k \right)^4 . \quad (15)$$

Inserting expression (15) into (13) and equating the linear terms relatively the variables

$$X \equiv x - \langle x \rangle, \; Y \equiv y - \langle y \rangle , \quad (16)$$

to zero, we obtain the following combination

$$K(X,Y) = K_2(X,Y) + K_4(X,Y) = I_4.$$
$$K_2(X,Y) = A_2 X^2 - 2B_2 X \cdot Y + C_2 Y^2,$$
$$K_4(X,Y) = A_4 X^4 - 2B_4 X^2 Y^2 + C_4 Y^4,$$
$$I_4 = A_4 \left\langle (\Delta x)^4 \right\rangle - 2B_4 \left\langle (\Delta x)^2 (\Delta y)^2 \right\rangle + C_4 \left\langle (\Delta y)^4 \right\rangle. \quad (17)$$

The following combinations shown below define the constants figuring in the DGI (17)

$$B_4 = \frac{\left\langle (\Delta x)^3 \right\rangle}{\left\langle (\Delta x)(\Delta y)^2 \right\rangle} A_4 \equiv \sigma_B A_4,$$

$$C_4 = \frac{\left\langle (\Delta x)^3 \right\rangle}{\left\langle (\Delta y)^3 \right\rangle} \frac{\left\langle (\Delta y)(\Delta x)^2 \right\rangle}{\left\langle (\Delta x)(\Delta y)^2 \right\rangle} A_4 \equiv \sigma_C A_4,$$

$$A_2 = \left[6 \left\langle (\Delta x)^2 \right\rangle - 2\sigma_B \left\langle (\Delta y)^2 \right\rangle \right] A_4 \equiv S_A A_4,$$

$$B_2 = 4\sigma_B \langle \Delta x \Delta y \rangle A_4 \equiv S_B A_4,$$

$$C_2 = \left[6\sigma_C \left\langle (\Delta y)^2 \right\rangle - 2\sigma_B \left\langle (\Delta x)^2 \right\rangle \right] A_4 \equiv S_C A_4. \quad (18)$$

The constant I_4 and *Inv* from (13) are defined by expression (19)

$$Inv = 2I_4 = 2\left[\left\langle(\Delta x)^4\right\rangle - 2\sigma_B\left\langle(\Delta x)^2(\Delta y)^2\right\rangle + \sigma_C\left\langle(\Delta y)^4\right\rangle\right]A_4. \quad (19)$$

The averaged values $\langle(\Delta x)^q(\Delta y)^p\rangle$ characterizing two comparing sets are defined by expressions (14). The curve $K(X,Y)$ can be separated in the polar coordinate system. Using the notations (16) and taking into account the fact that constant A_4 figuring in $K(X,Y)$ is the proportion multiplier and therefore can be omitted, we present the desired curve in the form

$$\begin{aligned} x(\varphi) &= \langle x\rangle + r(\varphi)\cos\varphi, \\ y(\varphi) &= \langle y\rangle + r(\varphi)\sin\varphi, \\ r(\varphi) &= \left[\frac{\sqrt{q_2^2(\varphi) + 4I_4 q_4(\varphi)} - q_2(\varphi)}{2q_4(\varphi)}\right]^{1/2}. \end{aligned} \quad (20)$$

The functions $q_{2,4}(\varphi)$ figuring in (20) are determined by expressions

$$\begin{aligned} q_2(\varphi) &= S_A\cos^2(\varphi) - 2S_B\sin\varphi\cos\varphi + S_C\sin^2(\varphi), \\ q_4(\varphi) &= \cos^4(\varphi) - 2\sigma_B\sin^2\varphi\cos^2\varphi + \sigma_C\sin^4(\varphi). \end{aligned} \quad (21)$$

This curve of the 4th order containing 8 statistical parameters ($\langle x\rangle$, $\langle y\rangle$, σ_B, σ_C, $S_{A,B,C}$, I_4) determines statistical proximity/difference between 2D random curves/sets located in the plane. What is happened if two random curves are identical with each other ($x_j=y_j$) for all numbers of the discrete points j=1,2,…,N?. In this case as it is easy to see from expressions (18) $\sigma_B = \sigma_C = 1$, $I_4 = 0$, $S_{A,B,C} = 4\langle(\Delta x)^2\rangle$ and, therefore, from (20), it follows that $r(\varphi) = 0$. In this case, expression (20) is degenerated into a *point* with coordinates $\langle x\rangle = \langle y\rangle$ located on the line $y=x$.

We want to stress here that the algorithm proposed in this paper is *original* and differs from the mathematical proofs that are given in the abovementioned book.

2.3 *The statistics of the fractional moments and the usage of the internal correlation factor*

The generalized Pearson correlation (GPC)-function was used earlier in the papers [13, 14] and it is defined as

$$GPC_p = \frac{GMV_p(s_1, s_2)}{\sqrt{GMV_p(s_1, s_1)\ GMV_p(s_2, s_2)}}, \quad (22)$$

where the generalized mean value GMV-function of the K-th order is

$$GMV_p(s_1, s_2, \ldots, s_K) = \left(\frac{1}{N}\sum_{j=1}^{N}\left|nrm_j(s_1)\, nrm_j(s_2)\cdots nrm_j(s_K)\right|^{mom_p}\right)^{\frac{1}{mom_p}}. \quad (23)$$

It employs the normalized sequences $nrm_j(y)$, with $0 < nrm_j(y) < 1$, and the current value of the moment, defined as mom_p. More specifically, for j = 1, 2,…,N, it holds:

$$nrm_j(y) = \frac{y_j - \min(y_j)}{\max(y_j - \min(y_j))}, \quad (24)$$

where y_j denotes the initial random sequence that can contain a trend or that is to be compared with another trendless sequence. The initial sequences are chosen like follows. The minimum of the GMV function is zero, while the maximum coincides with the maximum of the normalized sequence. Moreover, the set of moments is computed as follows:

$$mom_p = e^{L_{np}},\ L_{n_p} = mn + \left(\frac{p}{P}\right)(mx - mn) \quad p = 0, 1, \ldots, P \quad (25)$$

so that L_{n_p} takes values between (mn) and (mx) that define the limits of the moments in the *uniform* logarithmic scale. Usually, mn = –15, mx = 15, and 50 ≤P≤100. This choice is because the transition region of the random sequences that are expressed in the form of GMV-functions is usually concentrated in the interval [–10,10]. The extension to [–15,15] is considered for the accurate calculation of the limit values of the functions in the space of fractional moments. Finally note that GPC_p determined by (22) coincides with the conventional definition of the Pearson correlation coefficient at mom_p = 1.

If the limits (*mn*) and (*mx*) have the opposite signs and take sufficiently large values, then the GPCF has two plateaus (with $GPCF_{mn}$ =1 for small values of *mn*) and another limiting value GPC_{mx} that depends on the degree of internal correlation between the two compared random sequences. This right-hand limit, say *Lm*, satisfies the following condition:

$$M \equiv \min(GPC_p) \le Lm \equiv GPC_{mx} \le 1. \quad (26)$$

The appearance of two plateaus implies that all information about possible correlations is complete and a further increase of (*mn*) and (*mx*) is *useless*. Several tests showed that the highest degree of correlation between two random sequences is achieved when *Lm* = 1, while the lowest when *Lm* = *M*. For *quantitative* comparison of the internal correlations of two random sequences we introduce the following internal correlation factor (*ICF*)

$$ICF = M \cdot L. \quad (27)$$

Note that *ICF* is determined by using the total set of the fractional moments from the interval $[e^{mn}, e^{mx}]$. Putting (*mn*) = –15 and(*mx*) = 15, *ICF* tends to *M* for high correlation, and to M^2 for the lowest (remnant) degree of correlations. Moreover, *ICF* does *not* depend on the amplitudes of two compared random sequences. Since $0 \le |y_j| \le 1$ must hold for both sequences, (27) contains complete information about the internal correlations between the pair of the compared random sequences that is based on the similarity of probability distribution functions of the sequences, even if the last ones are usually *not* known.

Recently the statistics of the fractional moments was applied with promising results [13, 14], which gave the idea to use the *ICF* for unification of the significant parameters. Namely, for a set of significant parameters referring to one qualitative factor, it holds (note that always the parameter *M* < 1)

$$cf_{min} = M^2 \le ICF \le M, \quad (28)$$

where the low limit cf_{min} is determined by the sampling volume and the practical conditions of random sequences, that should be almost the same when comparing two different sequences, e.g. the first affected by a qualitative factor, the second by another factor like a control action.

Then, the clusterization method is based on comparing the values of the *ICF* factor, by making a sort of extension of the conventional method based on the Pearson correlation coefficient (PCC) that is not complete for detailed comparison of a pair of random sequences.

3. Electrochemical Application of the Method

3.1. *Experimental part*

All measurements were conducted with the use of potentiostat/galvanostat Elins-P30S (Chernogolovka, Russia) and three-electrode cell, where the glassy carbon rod as the counter electrode and Ag/AgCl (3.5 M KCl) electrode is used as the reference electrode. The graphite (C) and (Pt) electrodes were used as the working electrodes. The standard phosphate buffer solution (pH 6.86, the mixture Na_2HPO_4 and KH_2PO_4) was served as a background electrolyte. 1000 measurements were registered continuously with the constant stirring.

Each measurement cycle includes two stages:

1) Electrochemical regeneration – five successive cycling with the potential scan rate 2.5 V/sec.

2) Registration of VAG in the background electrolyte at the given potential scan rate 0.5 V/sec in the range of the potentials [0,1.5] V.

The cycling scheme of the current measurement is presented in Fig. 1.

3.2. *Description of the algorithm*

From experimental records, we obtained a set containing 1000 measurements and the obtained set was divided on 9 separate groups and each group, in turn, had 100 measurements (1-100, 101-200, 201-300, …,901-1000). The aim of this research is to

notice the surface modifications (possible aging tendencies) of each electrode (as it has been mentioned above we used Pt - and C-electrode, accordingly) that can be detected by electrodes during the extended experiment. However, before the proposing of an algorithm, we should find a definite and justified answer for the following question: *which curve is more sensitive for detection of possible electrode changings (a) differential curve (dJ/dU without trend or (b) the curve J(U) obtained after integration with trend?* For the finding of the definite answer, we use for comparison of two random curves with the help of the GPC-function (22) that is based on the complete set of the real moments and generalizes the conventional Pearson correlation coefficient. Therefore, we prepared initially the following data that allow to eliminate the influence of the remnant currents. The prepared data satisfy to the following requirements

$$Yn_m = \frac{DV_m(U) - \langle DV_m(U)\rangle}{stdev\left(DV_m(U) - \langle DV_m(U)\rangle\right)},$$
$$DY_m = Yn_m - \langle Yn_m\rangle,\ JY_m = Intergal\left(U, DY_m\right), \quad (29)$$
$$\langle DY\rangle_m = \frac{1}{M}\sum_{m=1}^{M} DY_m,\ \langle JY\rangle_m = \frac{1}{M}\sum_{m=1}^{M} JY_m.$$

Here parameter m=1,2…,M defines the number of the total measurements in one set (M=100) and measurement space, accordingly. $DV_m(U)$ – is initial data file refereed to the measurement m; the symbol <…> determines the arithmetic mean for each fixed measurement and is calculated in accordance with expression (14). Number of data points (j=1,2,…, N) for each measurement is equaled to N=1181 and any dependence from the applied potential U_j defines the data space. The symbol *Integral*(x,y) determines the conventional integral calculated by means of the recurrence trapezoid formula

$$Integral(x,y) \Rightarrow J_j = J_{j-1} + \frac{1}{2}\left(x_j - x_{j-1}\right)\cdot\left(y_{j-1} + y_j\right) \quad (30)$$

The final notions $\langle Y\rangle_m = M^{-1}\sum_m Y_m$ determine the couple of functions averaged over all measurements. This simple procedure helps to eliminate essentially the remnant currents and obtain the desired averaged curves that can be used for comparison of one set of a hundred measurements (d+1-d+100) (with d=0,100,200, …,900) with another one. The typical curves corresponding to comparison (1-100, 101-200) for Pt electrode are illustrated by the Figs 2(a,b) and Figs. 3(a,b) for the data (dJ/dU and J(U)) and measurements (DY_m and JY_m) spaces, correspondingly. Showing these figures we want to stress also another important fact, i.e., the curves in the data space given to respect of the applied potential have different sensitivity to the presence of the external factor in comparison with curves that show the range of the previous curves with respect to the number of measurements (m=1,2,…,M=100). The range of any random curve is defined by the conventional expression: Range(y)= max(y)-min(y). The differences between these curves expressed in the form of the GPC-functions (22) are shown in Figs. 4(a,b). The figures 5(a,b) demonstrate the behavior of the ICF for both types of the curves in data and measurement spaces, correspondingly. Analysis of these curves shows that with increasing of the duration of number of measurements (from 1 to 1000) the correlations between each hundred are diminishing. The correlation parameters of the DGIs of the second and the fourth order are shown in Fig. 6(a,b) and Fig. 7, correspondingly.

4. Results and Discussions

In order to understand better the results that were obtained in the frame of the DGIs parameters, we should remind to a potential reader some facts known earlier:

1. The receiving of the sensor stable response is important problem of the electroanalytical chemistry. Besides the mechanical cleaning of the sensor surface, its treatment by various

solutes and reagents the electrochemical regeneration of the sensor surface is applied. The electrochemical regeneration efficiency depends on the applied potential working range, the scanning rate, the content of the background electrolyte etc. For each specific case, the choice of the regeneration conditions has an empirical character. The direct control related to the state of the sensor/electrode surface is limited, especially in the routine analysis conditions. We note also that the low sensor sensitivity, its stability or the temporal drift cannot influence on the accuracy of the complete analysis.

2. In the case of nano-electroanalytics (it investigates a formation of different nanostructures on the electrode surface, chemical reaction of the solute components with nanoparticles located on the electrode surface and etc.) the final result depends strongly on the structure and nanostructures composition formed on the given electrode surface [15]. The results of electro-analysis have a practical importance in any case, but especially in cases, when the massive data are obtained in the long-time functioning sensors conditions. It has been established that the data obtained in the long-time conditions strongly depend on the material of the used electrode, in particular, the graphite (carbon C) exhibits more strong surface variations in comparison with platinum (Pt).

3. It was known that for modification of the graphite surface the electrochemical intercalation in various background electrolytes is used. In the result of this process application the following modifications are observed: (a) a partial carbon oxidation; (b) cavities opening between the layers of the graphite rings; (c) penetration of molecules and ions from the solutes inside the formed carbon cavities; (d) and formation of new chemical compositions with carbon. In the conditions of the realized experiment described in this paper, it leads to formation of some

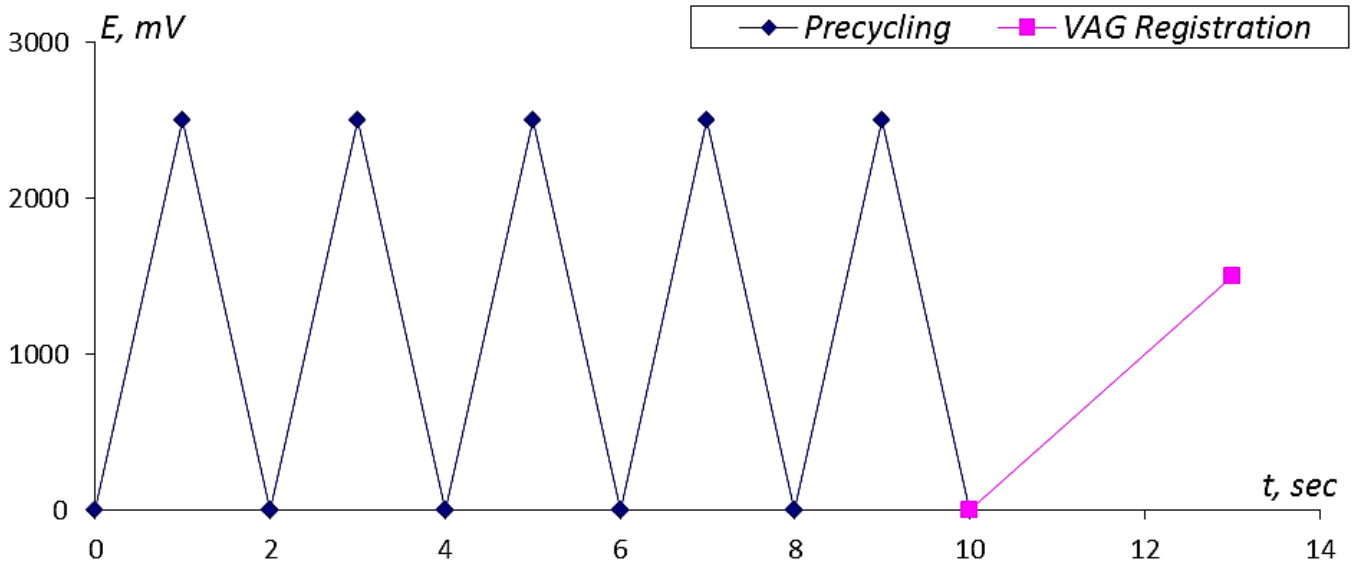

Fig. 1. The scheme of the measurement cycle. The time interval between measurements equals 10 sec. The period of the VAG registration occupies 3 sec.

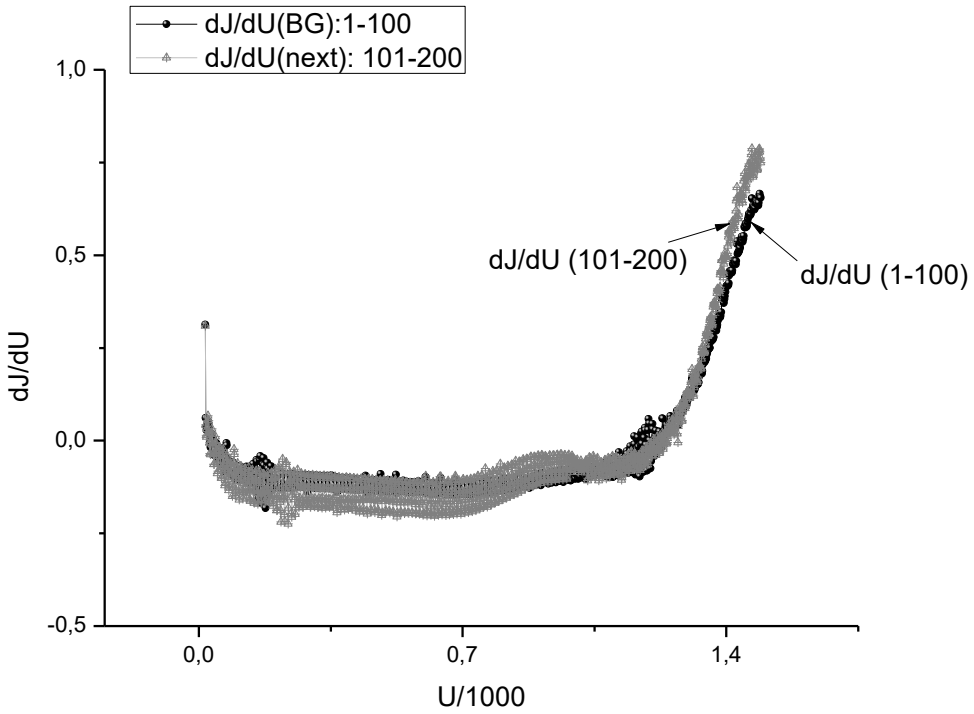

Fig.2(a). Initial data after elimination of the mean value, normalized for the standard deviation, and averaged over 100 measurements. See expression (29) for details.

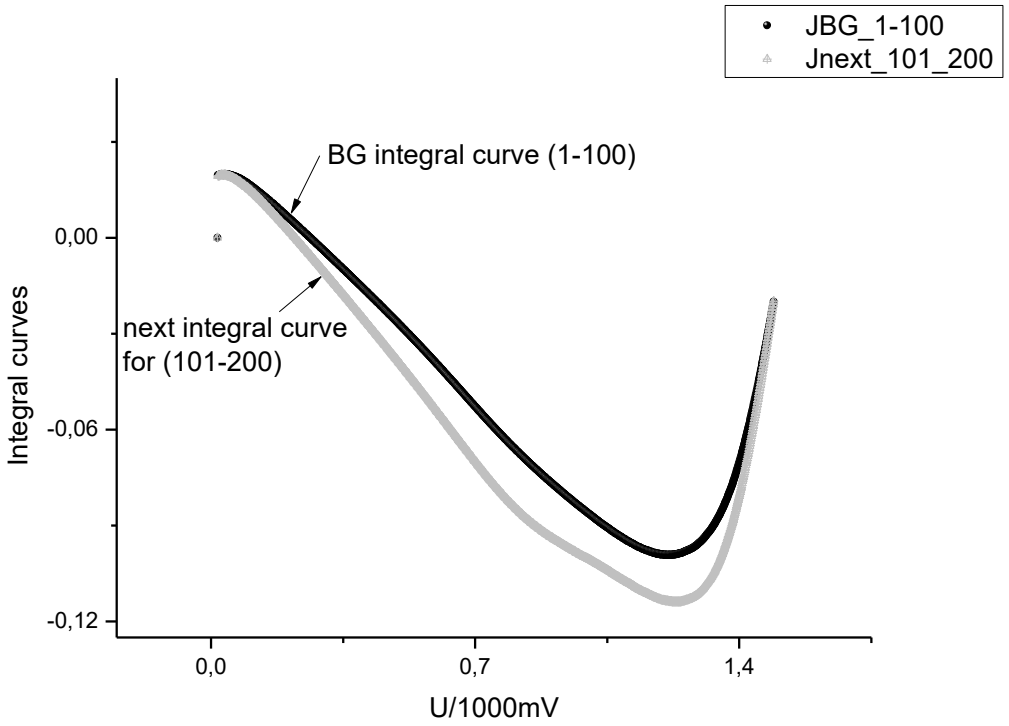

Fig. 2(b) The same curves after application of the mathematical manipulations (29) and subjected to the integration procedure. The differences between curves in comparison with initial curves shown in Fig.2(a) are expressed more clearly. The calculated correlations between these curves and expressed in the form of the ICFconfirm this visual observation quantitatively.

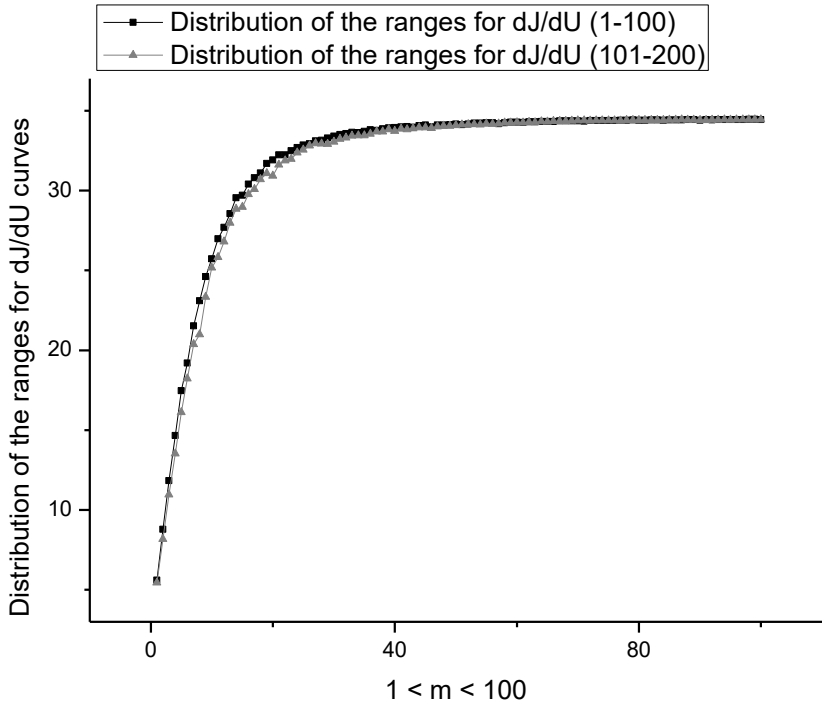

Fig.3(a). The behavior of the ranges of the curves depicted in Fig.2(a). As one can see from this figure the curves are monotone and close to each other. One can conclude that some process on Pt electrodes takes place.

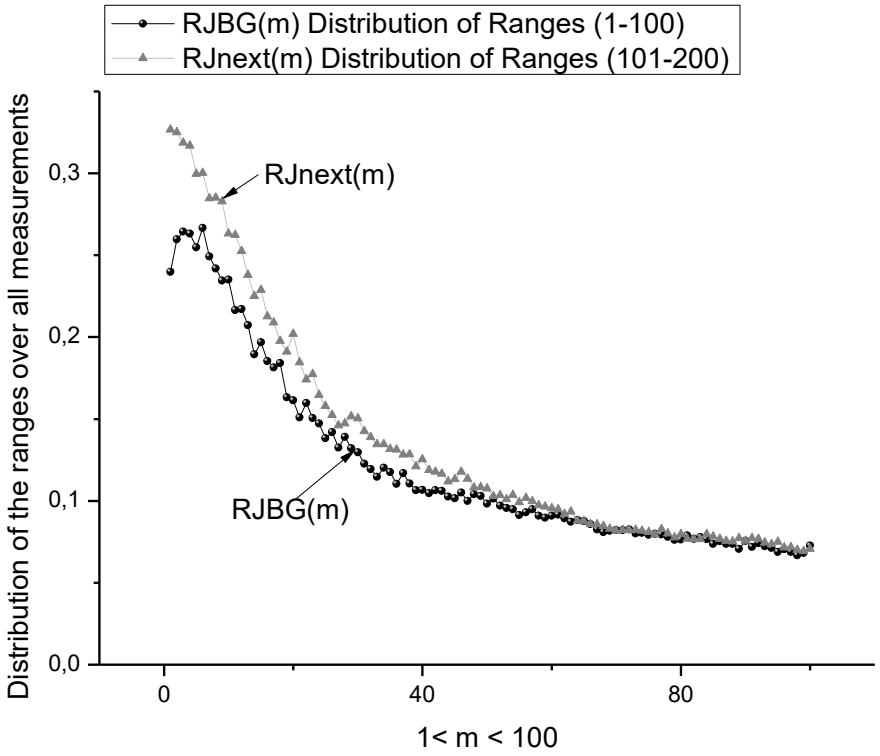

Fig.3(b). The comparison of the ranges for two integral curves shows that the ranges for integral curves are more deviated and, therefore, they can be used for detection of different additives, chemical electrode changing and influence of external factors, as temperature, pressure and etc.

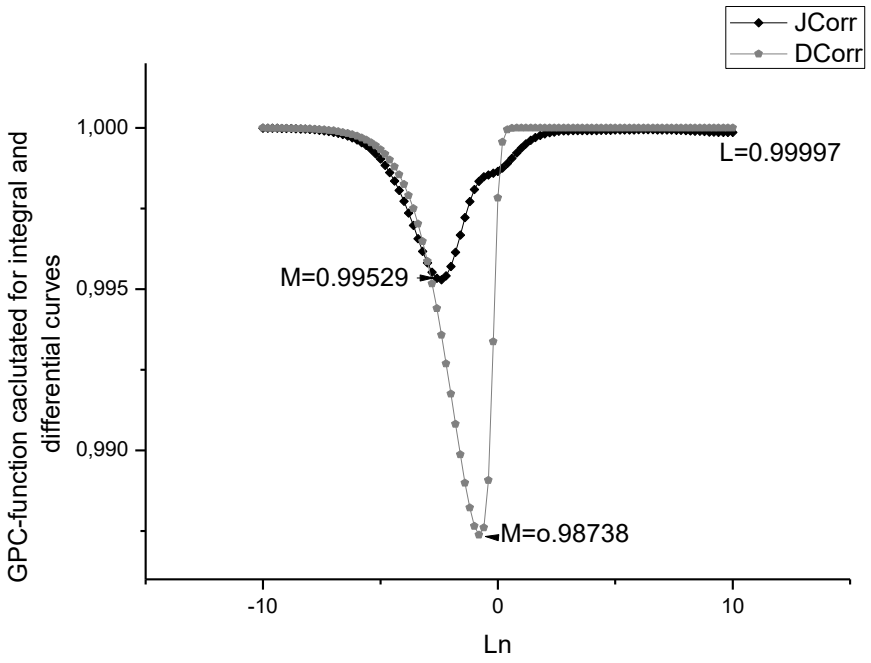

Fig.4(a). These curves demonstrate a typical behavior of the GPC-functions calculated for the curves shown above. Comparison of the two curves shows that the correlations for integral curves are stronger in comparison with correlations expressed for differential curves. But this tendency is not common, the comparison with other curves for measurements (201-300), …, (901-1000) show that correlations become weaken for integral curves with growing time in comparison with differential curves.

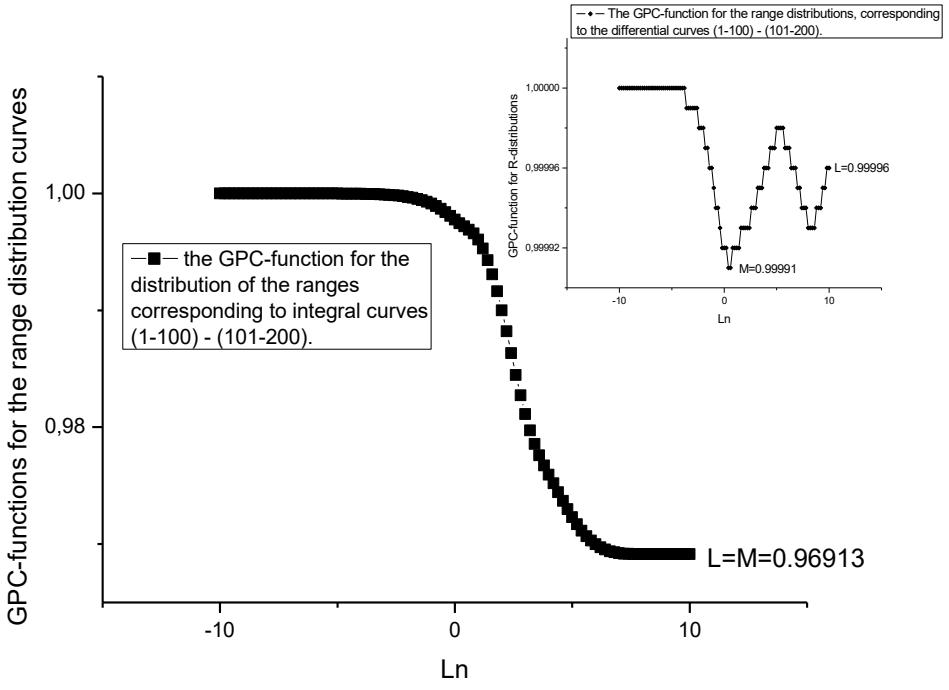

Fig.4(b). Comparison of the curves showing the range distributions for integral (central figure) and differential (small figure above) curves depicted in figures 3 demonstrates the opposite tendency. The correlation between integral curves weakens while for the differential curves one can observe the strong correlations located in the range 0.99991 <*ICF*< 1.0.

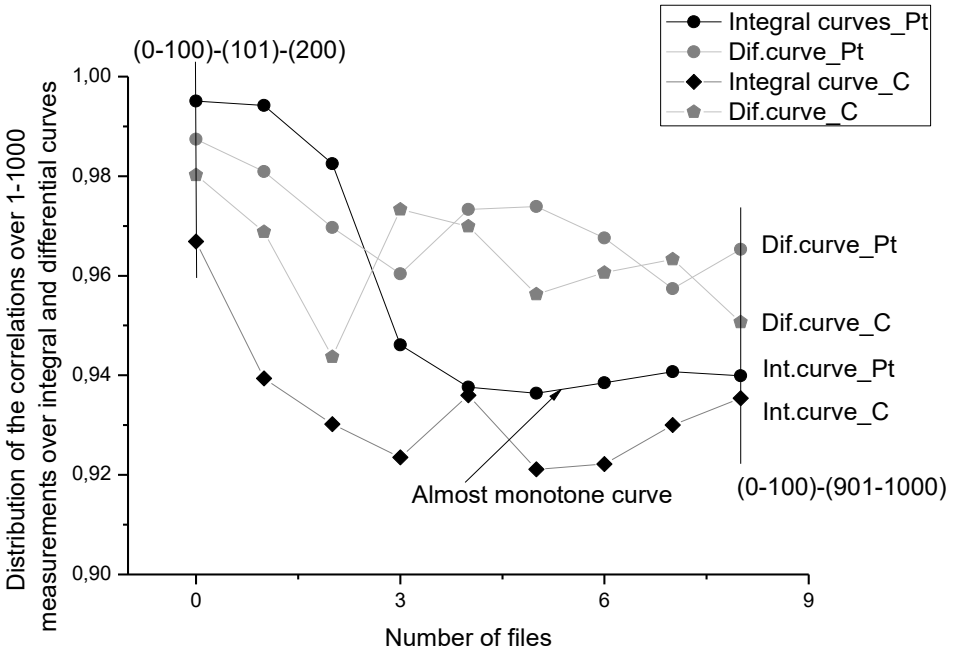

Fig.5(a). These plots demonstrate the different sensitivity of the integral and differential curves in the data space for all set of measurements covering the whole interval of measurements (1-1000). One can notice the general tendency hat is common for all curves, i.e. with increasing of time the correlation between measurement decreases. For integral curves, this tendency is stronger in comparison with differential curves. The almost monotone behavior belongs to integral curve for Pt electrode, while for carbon (C) electrode these correlations weaken and their behavior is not monotone.

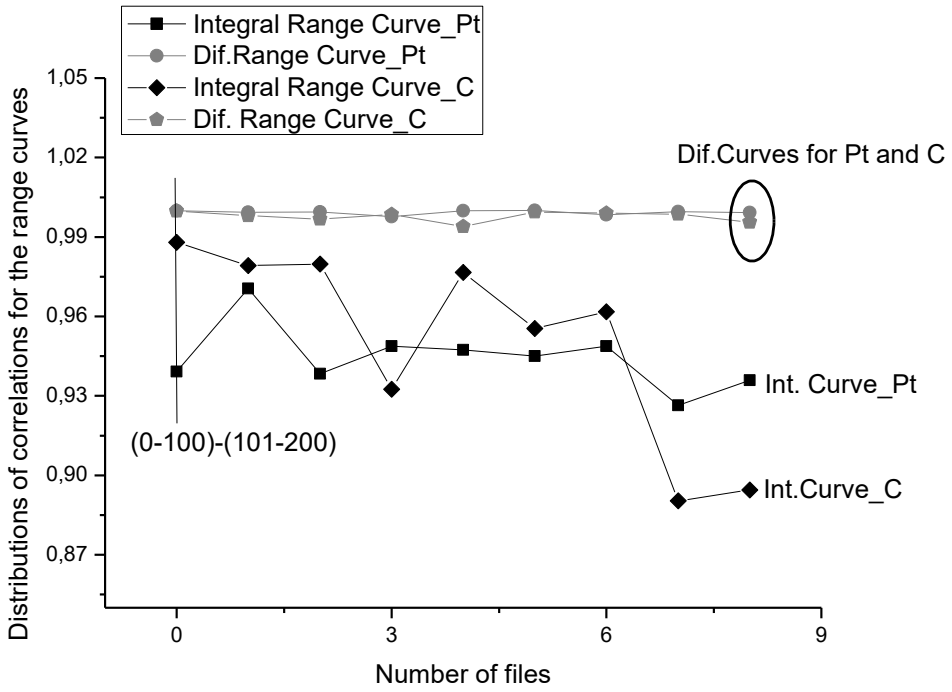

Fig.5(b). Here we plot the values of correlations for distribution of the ranges referring to integral and differential curves. The same tendency is observed, i.e. the correlations for integral curves weaken in comparison with the ranges distributions for differential curves however, this weakening correlation tendency is not monotone.

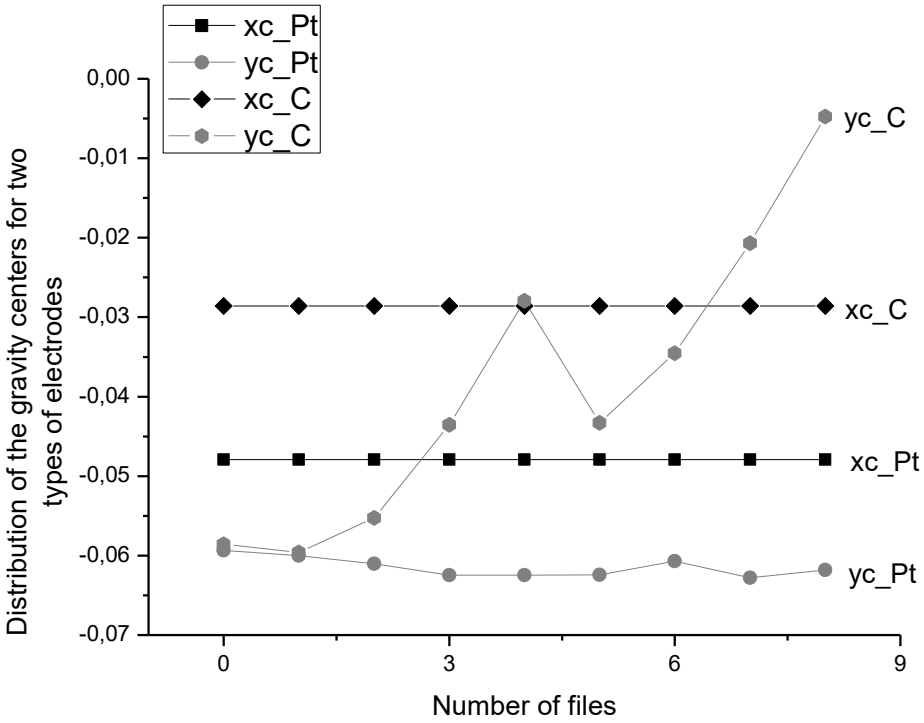

Fig.6(a). This figure demonstrates the parameters of the DGI of the second order (see expression (9)). As one can see from this figure the gravity centers $\langle x \rangle_{Pt,C}$for both ellipses remain constant, while the parameters $\langle y \rangle_{Pt,C}$ are changed. These changes for carbon (C) electrode are expressed more clearly and not monotone in comparison with the behavior of the gravity center $\langle y \rangle_{Pt}$ for Pt electrode (the lowest curve).

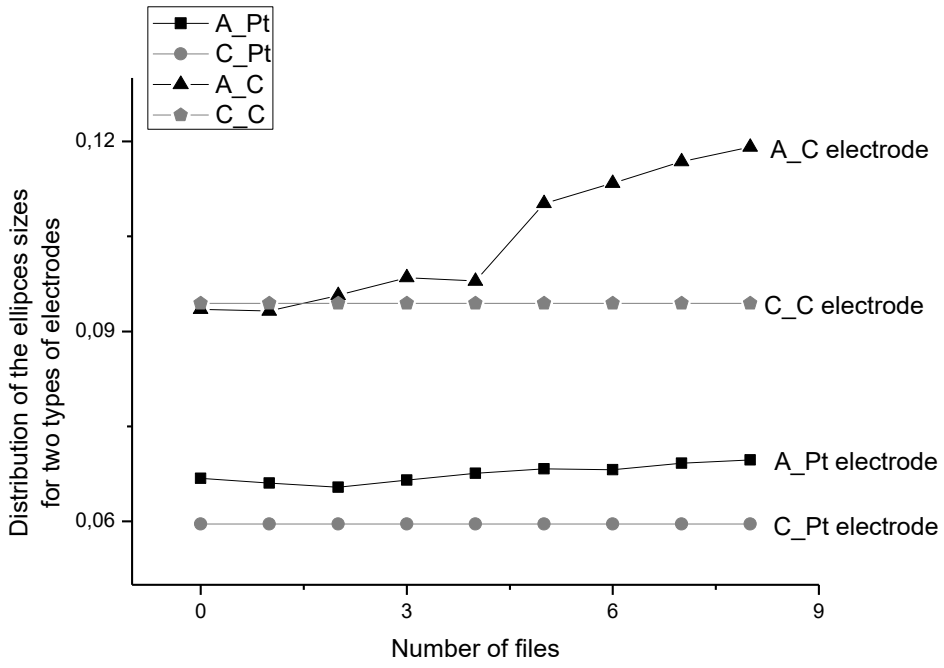

Fig.6(b). The behavior of the parameters *A* and *C* (see expressions (7) and (11)) characterizing the DGI of the second order. The parameters *C* for two types of electrodes remain constant, while the parameters *A* are changed. Again for C electrode these changes are expressed more clearly in comparison with C(Pt) electrode.

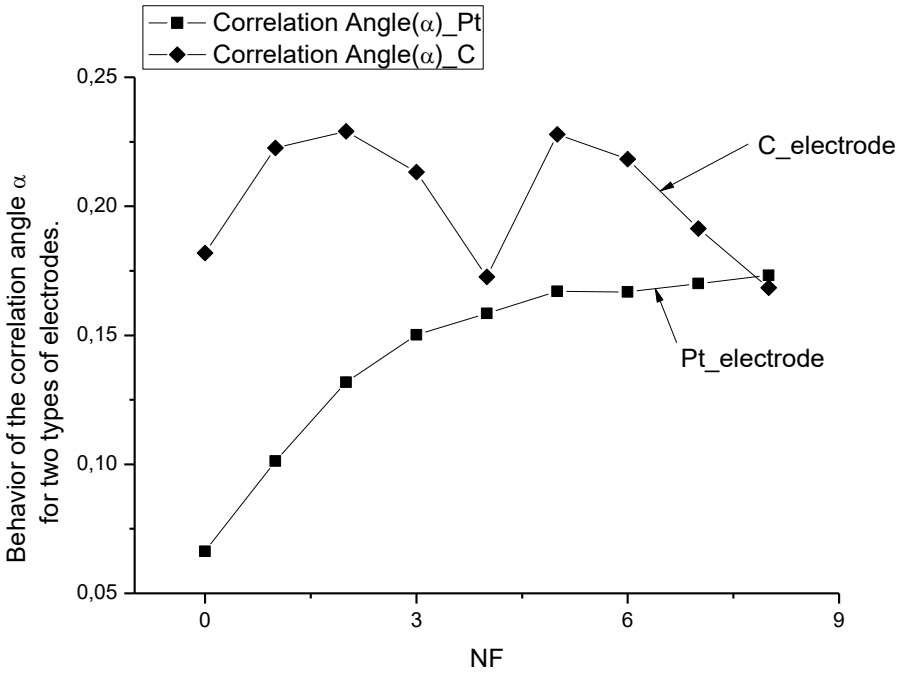

Fig.6(c) The behavior of the correlation angle α for two types of electrodes. This behavior is the most interesting in comparison with other plots. It demonstrates monotone behavior for the Pt-electrode while for the C-electrode this behavior is not monotone and more miscorrelated. This angle (in share of radians) is counted off relatively the angle $\pi/4$ in clockwise direction formed by the curve $Y=X$.

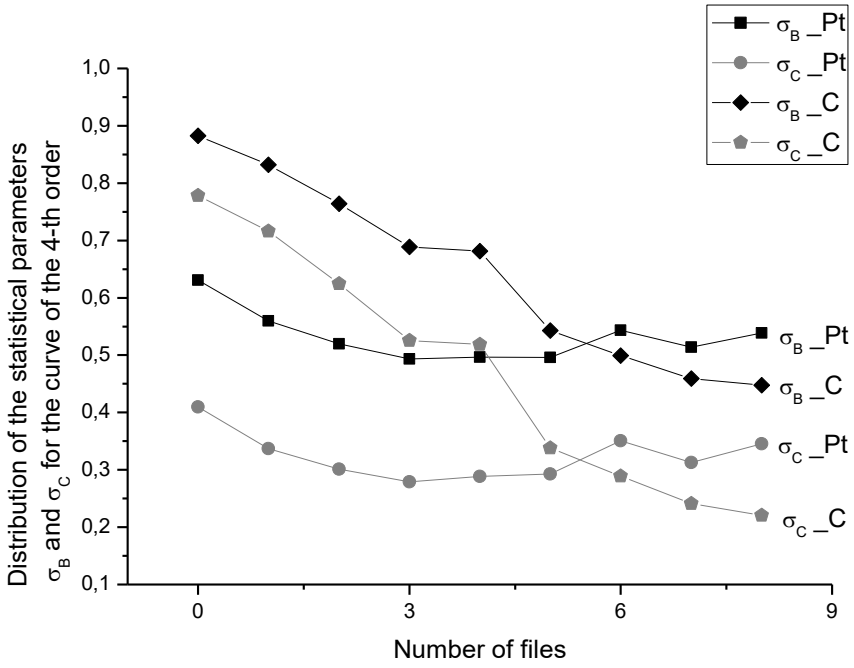

Fig.7. Here we show the behavior of the parameters $\sigma_{B,C}$ (defined by expressions (18)) of the DGI of the 4-th order. As preliminary analysis shows that these parameters are the most sensitive to possible changings of the presence of electrodes (Pt,C) in the given solution. If the sequences are strongly correlated then these parameters tend to the unit value. Again, we observe the weakening correlation phenomenon that is observed for all these parameters analyzed. The quasi-monotone behavior is observed for the parameters $\sigma_{B,C}$ corresponding to the carbon (C) electrode.

regions where the registered signal changes monotonically and sharp cross breaks on dynamical curves, where the formed graphite structure can be abruptly changed. These changes for carbon electrodes are noticeable also on Figs.6(a,b,c) which track the quantitative parameters belonging to the DGI of the second order. In Fig.7, they are also noticeable, especially in case when the background set (0-100) is compared with the set (401-500). This noticeable cross break in the same region is appeared on all the corresponding curves characterizing the behavior of C-electrode also in Figs.6(a,b,c).

4. In comparison with C-electrode the Pt – electrode is the chemically inert material. The basic changes take place on the metal surface of Pt. In the result of electro chemical input one obtains the oxygen and hydrate films with implantation of molecules and ions from the background electrolyte. On the surface of C-electrode, one observes a constant changing of the graphite layers that are chemically modified with the increasing of a distance from the initial layer while on the Pt-electrode one observes the growth of the dense film formed from the oxygen and hydrate atoms reacted with pure Pt surface. In the result of 1000-fold activation cycles, the surface of the C-electrode becomes loose while for the Pt-surface one observes the opposite tendency, i.e. the dense film is formed without essential modification of the Pt-electrode structure [16, 17]. It is interesting to note that the formation of the oxide film is monotone in time. This fact is confirmed by the curves depicted in Figs. (6,7) and referred to the Pt-electrode.

Finishing this final section, one can say the following. With the help of the proposed approach, one can detect quantitatively all qualitative changes of the analyzed VAGs, detect monotone regions and select the cross breaks regions, where the abrupt surface changings are possible. For this purpose, one can use the quantitative parameters of the DGI of the second order ($<x>$, $<y>$, A, C, α) (see expressions (9) and (10) above) and the most sensitive parameters as $\sigma_{B,C}$ defined by expression (18) and belonging to the DGI of the 4-th order. Besides of their application in electrochemistry, this general approach can be used for quantitative comparison of any couple of random sets located in 2D-plane. The authors do hope that this approach can find its proper place in various physical and chemical applications.

Acknowledgement

This work was supported by the Russian Foundation for Basic Research, project № 17-43-020232 r-Povolzh'ye-a.

References

[1] F. Scholz (Ed.), Electroanalytical Methods, Guide to Experiments and Applications, Springer-Verlag Berlin Heidelberg, 2002

[2] R.G. Compton, C.E. Banks, Understanding voltammetry, Second edition, Imperial College Press, 2011

[3] D.L. Massart, B.G. Vandeginste, L.M.C. Buydens, S. De Jong, P.J. Lewi, J. Smeyers-Verbeke, Handbook of Chemometrics and Qualimetrics: Part A, Amsterdam, Elsevier, 1997

[4] B.G. Vandeginste, D.L. Massart, L.M.C. Buydens, S. De Jong, P.J. Lewi, J. Smeyers-Verbeke, Handbook of Chemometrics and Qualimetrics :Part B, Amsterdam, Elsevier, 1998

[5] G. Henze, Polarographie und Voltammetrie, Springer-Verlag Berlin Heidelberg, 2001

[6] Holmin S., Krantz-Rülcker C., Lundström I., Winquist F., Measurement Science and Technology, 2001, 12 (8), 1348–1354

[7] Nigmatullin R.R., Budnikov H.C., Sidelnikov A.V. Electroanalysis, 2015, 27 (6), 1416–1426

[8] Nigmatullin R.R., Budnikov H.C., Sidelnikov A.V., Yarkaeva Y.A. New Journal of Chemistry, 2017, 41 (7), 2561–2573

[9] Nigmatullin R.R., Budnikov H.K., Sidelnikov A.V., Maksyutova E.I. Computer Communication & Collaboration, 2017, 5 (3), 12–32.

[10] Chesnokov N.V., Kuznetsov B.N., Mikova N.M. Journal of Siberian Federal University: Chemistry, 2013, 6 (1), 11–22

[11] Yu. I. Babenko. Power relations in a circumference and a sphere, USA: Norell Press Inc., 1997.

[12] Yu.I. BabenkoThe power law invariants od the point sets. Professional, S-Petersburg, ISBN 978-5-91259-095-5, www. naukaspb.ru, (Russian Feeration), 2014.

[13] Nigmatullin R.R., Ceglie C., Maione G., Striccoli D. Nonlinear Dynamics, 2015, 80 (4), 1869–1882.

[14] Nigmatullin R.R., Giniatullin R.A., Skorinkin A.I. Computational Neuroscience, 2014, 8, 120, DOI: 10.3389/fncom.2014.00120

[15] Budnikov H.C., Shirokova V.I. Journal of analytical chemistry, 2013, 68 (8), 663–670.

[16] B.B. Damaskin, O.A. Petrii, V.V. Batrakov, Adsorption of Organic Compounds on Electrodes, New York: Plenum Press, 1971.

[17] B.B. Damaskin, The Principles of Current Methods for the Study of Electrochemical Reactions, New York: McGraw-Hill, 1967.